rydbergs or 27.21 eV (hartree unit).
[8]I. Lindgren, Phys. Letters 19, 382 (1965); Arkiv Fysik 31, 59 (1966); E. A. Kmetko, Phys. Rev. A 1, 37 (1970); J. H. Wood, Intern. J. Quantum Chem. 35, 747 (1970).
[9]T. M. Wilson, J. H. Wood, and J. C. Slater, Phys. Rev. A 2, 620 (1970); K. Schwarz (unpublished).
[10]M. Berrondo and O. Goscinski, Phys. Rev. 184, 10 (1969).
[11]I. Lindgren, Intern. J. Quantum Chem. S5 (1971); I. Lindgren and A. Rosén (unpublished).

PHYSICAL REVIEW A VOLUME 5, NUMBER 2 FEBRUARY 1972

g_J Values of the $5d[\frac{7}{2}]_{4,3}$ and $5d[\frac{3}{2}]_2$ States in Xe and Hyperfine Structure of the $5d[\frac{7}{2}]_4$ State in ^{129}Xe†

Michael H. Prior and Charles E. Johnson
Department of Physics and Lawrence Berkeley Laboratory, University of California, Berkeley, California 94720
(Received 4 October 1971)

A magnetic-resonance technique has been used to make an accurate measurement of the g_J values of the $5d[\frac{7}{2}]_4$, $5d[\frac{7}{2}]_3$, and $5d[\frac{3}{2}]_2$ states in xenon and of the hyperfine structure of the $5d[\frac{7}{2}]_4$ state in ^{129}Xe. The $5d$ states are excited and aligned by unidirectional electron impact in a hot-cathode discharge tube containing Xe at a pressure of about 5×10^{-3} Torr. Induced transitions between magnetic sublevels of the aligned $5d$ state are detected by monitoring the intensity of linearly polarized light emitted during the second step in the cascade $5d\rightarrow6p\rightarrow6s$. The g_J values were measured by determining the Zeeman transition frequency of a particular $5d$ state in a magnetic field of about 20 G which had been locked to the Zeeman resonance in the $6s[\frac{3}{2}]_2$ metastable state. The results are $g_J=1.2506(3)$ for $5d[\frac{7}{2}]_4$, $g_J=1.0749(4)$ for $5d[\frac{7}{2}]_3$, and $g_J=1.3750(3)$ for $5d[\frac{3}{2}]_2$. The hyperfine structure was measured by placing the tube in a TE_{102} microwave cavity and observing direct ($\Delta F=1$) hyperfine transitions in a magnetic field of a few gauss. The result for ^{129}Xe in the $5d[\frac{7}{2}]_4$ state is $a=-583.571(2)$ MHz. The error for both the g_J values and the hyperfine structure arises from the magnetic field measurement and corresponds to about one-tenth of the linewidth. Our results are improvements of previous optical measurements.

I. INTRODUCTION

Many of the states with $J\neq1$ arising from the $5p^5\,5d$ configuration in xenon have relatively long radiative lifetimes ($\geq10^{-5}$ sec). This is due to the nearness (≈2000 cm^{-1}) of the $5p^5\,6p$ states to which they decay. Their long lifetimes allow the build-up of large population inversions, which account for the strong infrared laser lines connecting the $5d$ and $6p$ states. In this experiment we have taken advantage of these long lifetimes to make precision magnetic-resonance studies of three $5d$ states: $5d[\frac{7}{2}]J=4$, $5d[\frac{7}{2}]J=3$, and $5d[\frac{3}{2}]J=2$. The technique used is that of magnetic resonance following electron-impact excitation and alignment. This method was first demonstrated by Dehmelt[1] using Hg and was extensively applied to the study of He by Lamb and co-workers.[2] Since these pioneering investigations, the technqiue has been used to study the excited states of many atoms as well as a few ions and molecules; much of this work has been summarized by Pebay-Peyroula.[3] The $7p[\frac{3}{2}]_2$ and $7p[\frac{5}{2}]_3$ states of xenon have been studied by Chenevier[4] using this technique.

In particular, we have measured the Landé g factors for the three $5d$ states listed above and also the hyperfine structure (hfs) of the $5d[\frac{7}{2}]_4$ state in ^{129}Xe ($I=1/2$). Our results represent improvements of previous optical measurements of the hfs by Liberman,[5] and of the g_J values by Schlossberg and Javan.[6]

II. METHOD

The Xe energy levels relevant to this experiment are shown in Fig. 1. It is seen that the $5p^5\,5d$ states can be produced by electron bombardment with a threshold of about 10 eV. For illustrating the technique, we can limit discussion to the $5d[\frac{7}{2}]_4$ state. The decay path for this state is the two-photon cascade $5d[\frac{7}{2}]_4\rightarrow6p[\frac{5}{2}]_3\rightarrow6s[\frac{3}{2}]_2$ with $\lambda_1=55\,750$ Å and $\lambda_2=8819$ Å. As is known,[3] unidirectional electron bombardment near threshold produces an aligned excited state, i.e., Zeeman sublevels with different $|m_J|$, have different probabilities of excitation and consequently different populations. Following excitation, this alignment manifests itself in the polarization and anisotropy of the decay radiation. Since alignment is transferred to the intermediate state by the first step in the cascade, radiation emitted in the second step will also exhibit polarization and anisotropy. Therefore, changes in the populations of the $5d$

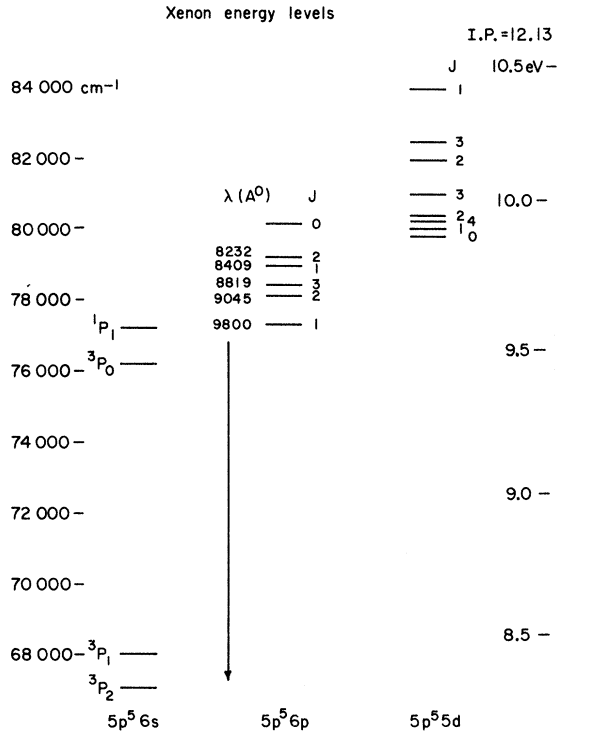

FIG. 1. Xenon energy-level diagram showing the lowest-lying levels. The $5p^5 5d$ states are produced by electron bombardment. The $J=4$ and the lower $J=3$, 2 states are those studied in this experiment. Decay is via the $6p$ levels to the $6s$ levels.

Zeeman sublevels induced by magnetic resonance can be observed by monitoring the resultant change in the polarization of the radiation emitted in the second step of the cascade. To establish a splitting of the Zeeman levels, an external magnetic field is applied parallel to the electron-impact direction. The magnetic resonances are obtained by linearly varying either the applied frequency or the magnetic field.

Since more than one decay path is available for the $5d[\frac{7}{2}]_3$ and $5d[\frac{3}{2}]_2$ states, the decay scheme is not as simple as that for the $5d[\frac{7}{2}]_4$ state. The $J=3$ state may decay by three different routes to the $6s[\frac{3}{2}]_2$ state, yielding second-step photons with wavelengths 8819, 8232, and 9045 Å. Decay of the $5d[\frac{3}{2}]_2$ state yields in addition photons with $\lambda = 8409$ and 9800 Å. In principle, observation of any of these wavelengths could be used to detect changes in the initial-state alignment caused by magnetic resonance. However, variations of the initial population distribution among the $5d$ Zeeman sublevels, the relative transition probabilities to the intermediate- and final-state sublevels, and the efficiency of detection of the second step intensity and polarization imply that the strength of the resonance signal depends upon which wavelength is observed.

We found that, under our operating conditions, the best signal-to-noise ratios were obtained on resonances in the $5d$ $J=4$, 3, and 2 states while observing the lines at $\lambda = 8819$, 9045, and 8232 Å, respectively. One could monitor several (or indeed all) second step lines; however, since some of the lines exhibit opposite polarization changes on resonance, the net signal-to-noise might not be increased and in fact could well decrease, unless this were compensated for in the detection system. We found that observing just one line was adequate.

Except when operating just above threshold with a monoenergetic electron beam, it is difficult to predict the exact population distribution among the excited-state Zeeman sublevels. This is because the relative excitation cross sections to the different m_J states are not known; moreover, as the electron-impact energy increases above threshold, cascading from higher-lying states becomes important. However, to observe the magnetic-resonance signals, it is not necessary to know precisely the initial-state alignment, but only that some alignment exists.

In addition to the three $5d$ states, resonance signals were observed in the $6s[\frac{3}{2}]_2$ metastable state. Since its g_J has been precisely measured[7] by the molecular-beam magnetic-resonance technique, resonance signals in this state of the even-mass Xe isotopes serve as a convenient means of calibrating and locking the magnetic field. This calibration resonance was easily observed for all of the monitored lines: $\lambda = 8819$, 9045, and 8232 Å.

III. APPARATUS

Figure 2 shows the hot-cathode discharge tube used in this experiment. The indirectly heated cathode is a $\frac{1}{2}$-in.-diam $\frac{1}{16}$-in.-thick porous tungsten disk impregnated with barium oxide.[8] A tantalum heat shield surrounds both the cathode and the heating filament; the anode is also constructed of tantalum. The cathode assembly is mounted on a commerical 7-pin tube base which has tungsten pins. The cathode-to-anode spacing is 1.25 in., which matches the narrow inside dimension of the waveguide cavity used in the ^{129}Xe hfs measurement.

After assembly, primarily spot welding, the tube was attached to an all-glass diffusion-pumped vacuum system and outgassed by a combination of induction heating the metal parts to 800–1000 °C and baking the glass envelope and tubulation at 300 °C. With the pressure in the tube maintained at less than 10^{-6} Torr, the cathode was activated by heating it to about 1200 °C until a steady emission of several mA at 100 V was obtained. After cooling the glass envelope and metal parts, but with the cathode at its operating temperature of about 1000 °C, the pressure in the tube was less than 10^{-7} Torr. The

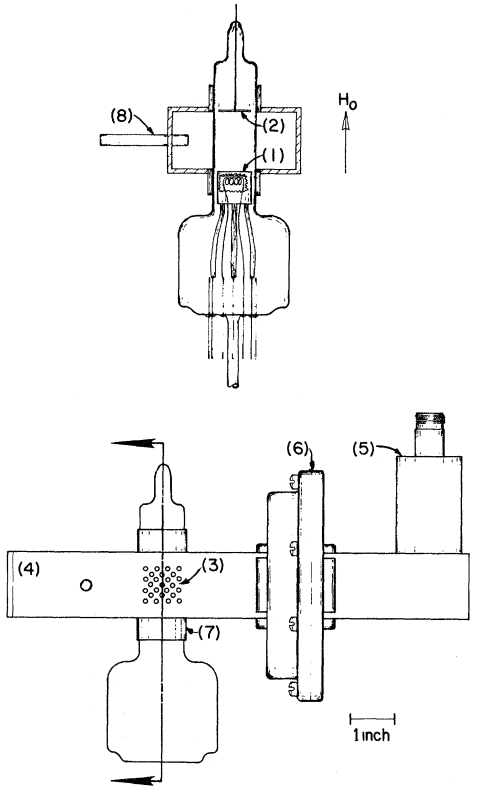

FIG. 2. Hot-cathode discharge tube and rf cavity. The cathode (1) is indirectly heated and surrounded by a Ta heat shield. Electrons accelerated towards the anode (2) produce a discharge which is viewed through holes (3) in the side wall of the TE_{102} mode cavity (4). The rf power is coupled to the cavity through a waveguide to type-N adapter (5) and circular iris (6). Radiation chokes (7) help preserve the cavity Q. The cavity is tuned using the quartz tuning rod (8) to the frequency appropriate for inducing direct ($\Delta F = 1$) hyperfine transitions in ^{129}Xe. For the g_J measurements, rf coils replaced the cavity.

tube was left attached to the vacuum-gas handling system to allow the xenon pressure to be varied as well as to permit reactivating the barium oxide cathode should it become poisoned, as it occasionally did.

During operation the cathode-to-anode potential was typically 20 V and the emission current limited to 120 mA.. This high emission at low voltage is due to the neutralization of the electron space charge by xenon ions. Under these conditions, most of the cathode-to-anode gap was filled with a field-free plasma; the electrons gained all of their energy in passing through a thin (0.5 mm) dark sheath just above the cathode surface. It was in the plasma region that most of the Xe excitation took place and from which the decay radiation was observed.

Figure 3 shows the over-all experimental arrangement and data-collection system. An external magnetic field H_0 parallel to the electron-impact direction was generated by a pair of 50-cm-diam Helmholtz coils which were energized by a programmable constant current power supply; the programmable feature allowed the magnetic field to be easily swept. An oscillatory rf field H_{rf} perpendicular to the external magnetic field was supplied by a pair of small coils for the g_J measurements, and by a TE_{102} cavity for the hfs measurement. In both cases, the rf field was square-wave modulated at 200 Hz for lock-in detection of the resonance signal; the current through the filament indirectly heating the cathode was pulsed at 400 Hz to prevent this current from influencing the observed resonance. The particular $6p \rightarrow 6s$ line being monitored was isolated by means of 20-Å-bandpass interference filters. Two photomultipliers (RCA 7102) and linear polarizers were used to monitor the intensity of light polarized both parallel and perpendicular to H_0. This arrangement greatly improves the signal-to-noise ratio since the resonance signal has opposite sign, but the noise does not, for the two polarizations; therefore, a differential amplifier reduces the background while adding together the signals. At resonance the parallel and perpendicular polarization intensities contain 200-Hz alternating components of opposite phase due to the modulated rf mixing of the $5d$ Zeeman sublevels. This modulated signal is detected by a Princeton Applied Research Co. HR-8 lock-in amplifier. The dc output of the HR-8 is converted to a pulse rate by a Vidar Model 260 voltage to frequency converter; these output pulses are then counted and stored in a RIDL 400-channel analyzer used in the multichannel scalar mode. The analyzer channel-address

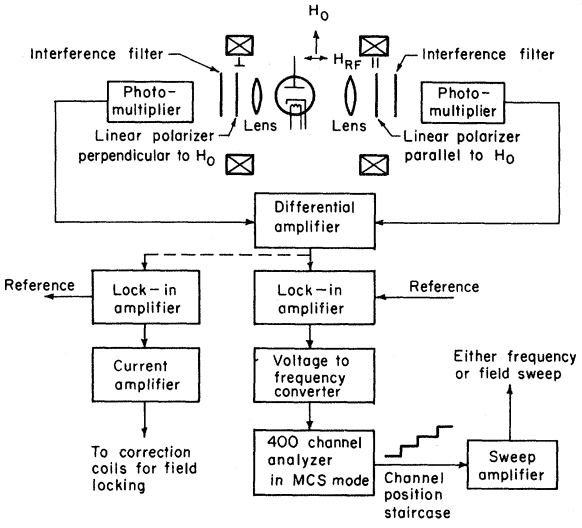

FIG. 3. Outline of the apparatus and data-collection system.

output-voltage staircase is used either to sweep the magnetic field or the applied rf frequency. The dwell time in any one channel can be controlled via a variable time base generator. The total number of sweeps through the analyzer memory can be preset or allowed to increase until terminated. This system is a sensitive differential signal averager which can collect resonance signals versus either magnetic field or rf frequency.

IV. STUDY OF LINEWIDTHS vs PRESSURE

The resonance linewidth Γ (full width at half-maximum) observed in this experiment is given by

$$\pi\Gamma = \frac{1}{T_r} + \pi\Gamma_0 + kP_{rf} \ ,$$

with (1)

$$\pi\Gamma_0 = \frac{1}{\tau} + \frac{1}{T_W} + g_J \frac{\mu_B}{h} \langle \Delta H_0 \rangle \ ,$$

where T_r is the net two-body collision relaxation time of the excited-state alignment, τ is the natural lifetime of the excited state, T_W is the wall collision relaxation time, $\langle \Delta H_0 \rangle$ is the mean variation of the applied magnetic field averaged over the resonance region, and kP_{rf} is the broadening due to the rf power.

T_r may be expressed in terms of a collision cross section σ as

$$T_r^{-1} = n\sigma v \ , \quad (2)$$

where n is the density of xenon ground-state atoms, and v is the average relative velocity of the excited- and ground-state atoms. The total cross section $\sigma = \sigma_z + \sigma_x$ arises from two separate processes; σ_z is the cross section for collisional mixing of the Zeeman levels and σ_x is the cross section for collisional deexcitation of the excited state. The latter process is not at all efficient unless the net change in internal energy is small. This is the case for the $5d[\frac{7}{2}]_4$ state, which is only 200 cm^{-1} from the $5d[\frac{1}{2}]_1$ state and 126 cm^{-1} from the $5d[\frac{3}{2}]_2$ state. Deexcitation is less likely for the $6s[\frac{3}{2}]_2$ state, which is about 1000 cm^{-1} from the $6s[\frac{3}{2}]_1$ state.

We made a series of measurements of the resonance linewidth vs pressure for the $6s[\frac{3}{2}]_2$ and $5d[\frac{7}{2}]_4$ states of the even Xe isotopes to determine the relative values of σ for these two states. At each pressure, measurements were made for several values of rf power and then extrapolated to zero power. The pressure was varied over a range $1-15\times10^{-3}$ Torr and was measured by a trapped McLeod gauge. However, because of the known pumping effects in trapped McLeod gauges, which can lead to large errors, the gauge readings were not reliable as absolute values. The slopes of the straight lines fit to the linewidth-vs-pressure data yielded

$$\frac{d\Gamma}{dP}\left(5d[\tfrac{7}{2}]_4\right) = 13.6(14) \text{ MHz/Torr (McLeod)}$$

and

$$\frac{d\Gamma}{dP}\left(6s[\tfrac{3}{2}]_2\right) = 7.6(8) \text{ MHz/Torr (McLeod)} \ .$$

This gives for the relative relaxation cross sections

$$\frac{\sigma(5d[\frac{7}{2}]_4)}{\sigma(6s[\frac{3}{2}]_2)} = 1.8(3) \ .$$

The effective temperature in the resonance region is not known precisely but was about 400–500 K. The intercept ($P = 0$) of the straight lines yielded values for Γ_0 of

$$\Gamma_0(5d[\tfrac{7}{2}]_4) = 44(4) \text{ kHz} \ ,$$

$$\Gamma_0(6s[\tfrac{3}{2}]_2) = 8.4(8) \text{ kHz} \ .$$

Because the $6s[\frac{3}{2}]_2$ metastable state has a very long natural lifetime ($\tau > 1$ sec),[9] the value of Γ_0 for this state arises from T_W and the magnetic field inhomogeneity $\langle \Delta H_0 \rangle$. One may use the value of Γ_0 for the $5d[\frac{7}{2}]_4$ state to set a lower limit for the lifetime of this state; therefore from Eq. (1)

$$\tau(5d[\tfrac{7}{2}]_4) \geq (\pi\Gamma_0)^{-1} \geq 10 \ \mu\text{sec} \ .$$

V. g_J MEASUREMENTS

During the g_J measurements, the magnetic field was held constant while the rf frequency was swept. The swept rf source was a Hewlett Packard 5105 A frequency synthesizer. As shown in Fig. 3, a second lock-in system detecting resonance in the $6s[\frac{3}{2}]_2$ metastable state was used to hold the magnetic field constant. A second rf field, applied to the resonance region by an additional pair of rf coils orthogonal to the main set, was frequency modulated at 150 Hz. Therefore, the dc output of the second lock-in amplifier was a dispersion curve (derivative of the resonance line shape) and suitable for use as an error signal to control the current through a pair of field-correction Helmholtz coils. Any change in the applied field H_0 attempting to shift the $6s[\frac{3}{2}]_2$ locking resonance was compensated for by a suitable field produced by the error current through the field-correction Helmholtz coils. This field locking system was capable of holding the field constant to at least 2 parts in 10^5 during a data-collection period.

Figure 4 shows one of the resonance signals used to determine g_J of the $5d[\frac{7}{2}]_4$ state. For this resonance curve, the field was locked to 24.135 G corresponding to a $6s[\frac{3}{2}]_2$ resonance frequency $\nu_2 = 50.700$ MHz. The frequency for the $5d[\frac{7}{2}]_4$ resonance was swept over the range 42.500–42.000

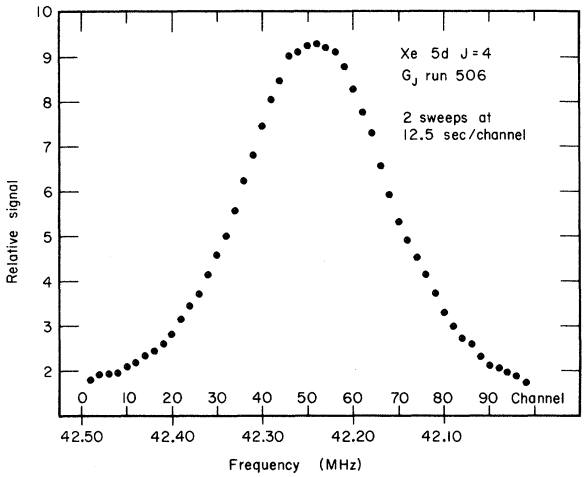

FIG. 4. Example of a g_J resonance.

MHz. The resonance curve was least-squares fitted to a Lorentzian line shape on a sloping baseline;

$$S(\nu)=\frac{A}{(\nu-\nu_0)^2+B}+C(\nu-\nu_0)+D\ . \tag{3}$$

The least-squares fit determined the best values for the five parameters ν_0, A, B, C, and D; ν_0 is the resonance center and $B^{1/2}$ is the half-width at half-height. The C and D terms in Eq. (3) were necessary to correct the sloping baseline introduced by a nonresonant effect of the modulated rf on the light intensity from the Xe discharge. This effect was dependent on the rf coupling to the plasma and hence varied slowly as the frequency was swept. The differential detection scheme reduced this effect enormously, but a small residual necessitated inclusion of the C and D terms.

The center of the resonance shown in Fig. 4 is $\nu_0 = 42.243$ MHz and the half-width at half-maximum $B^{1/2} = 0.120$ MHz. Each point in Fig. 4 is the result of 25 sec of averaging by the data-collection system. Many similar resonances were collected to determine the three g_J values; Table I summarizes all the data. The mean values of the separate measurements give our final results:

$$5d[\tfrac{7}{2}]_4,\quad g_J = 1.2506(3)\ ;$$

$$5d[\tfrac{7}{2}]_3,\quad g_J = 1.0749(4)\ ;$$

$$5d[\tfrac{3}{2}]_2,\quad g_J = 1.3750(3)\ .$$

The errors correspond to approximately one-tenth of the mean resonance half-width at half-maximum. These values are obtained from the data in Table I using the relation

$$g_J = g_2\,\nu_0/\nu_2\ , \tag{4}$$

where ν_0 is the $5d$ resonance line center, ν_2 is the $6s[\frac{3}{2}]_2$ field-locking frequency, and $g_2 = 1.5009(1)$ the g factor of the $6s[\frac{3}{2}]_2$ state.[7]

VI. $5d[\frac{7}{2}]_4$ hfs MEASUREMENT

Since ^{129}Xe is present in an abundance of 26.4%, we observed, in addition to the g_J resonances of the even-mass xenon isotopes, resonances with $\Delta F = 0$ between hyperfine Zeeman sublevels of the $5d[\frac{7}{2}]_4$ state of ^{129}Xe. Because the electron-impact excitation is much faster (10^{-14} sec) than the hfs period (10^{-10} sec), the initial alignment of this state of ^{129}Xe depends only upon $|m_J|$, as for the even isotopes. Immediately after the excitation collision, the alignment of the hyperfine sublevels (F, m_F) occurs through the coupling of the nuclear spin $\vec{I}$ with the electronic angular momentum $\vec{J}$ to form the total angular momentum $\vec{F}$. The Clebsch-Gordan coefficients which express (F, m_F) states in terms of (J, m_J, I, m_I) determine the alignment of the (F, m_F) sublevels corresponding to a particular initial $|m_J|$ alignment.

Figure 5 indicates the ^{129}Xe $5d[\frac{7}{2}]_4$ energy levels in a magnetic field. An initial excitation and alignment among the m_J states with $|m_J| = 0,\ 1,\ 2$ is assumed; the probability of excitation, and thus the initial population of these states, is proportional to the quantities α, β, γ. The resulting alignment of the (F, m_F) sublevels after coupling of $\vec{I}$ and $\vec{J}$ is

TABLE I. Summary of g_J measurements; $g_J(5d) = g_2\nu_0/\nu_2$, $g_2 = 1.5009(1)$.

State	No. of runs	Mean freq. ν_0 of resonance center (MHz)	Mean half-width at half-maximum (MHz)	$6s[\frac{3}{2}]_2$ field-lock freq. ν_2 (MHz)	Magnetic field (G)
$5d[\frac{7}{2}]_4$	15	42.244	0.089	50.700	24.135
$5d[\frac{7}{2}]_3$	9	32.591	0.151	45.500	21.660
	4	44.388	0.150	62.000	29.515
$5d[\frac{3}{2}]_2$	7	38.474	0.091	42.000	19.994
	4	55.418	0.098	60.500	28.800
	4	76.510	0.092	83.500	39.749

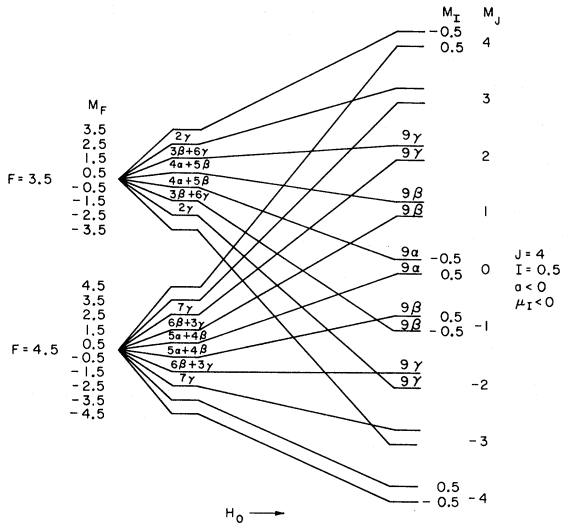

FIG. 5. Sketch of the hyperfine Zeeman sublevels of the $5d[\frac{7}{2}]_4$ state of ^{129}Xe.

then determined. Our observed resonance signals between (F, m_F) sublevels are consistent with the assumption $\alpha = \beta = \gamma$. These resonances were identified at low magnetic field by their effective g factor

$$g_F = \frac{g_J[F(F+1)+J(J+1)-I(I+1)]}{2F(F+1)} + \frac{g_I[F(F+1)+I(I+1)-J(J+1)]}{2F(F+1)} , \quad (5)$$

where $\vec{F} = \vec{I} + \vec{J}$ is the total angular momentum and $g_I = -8.415\times10^{-4}$ is the nuclear g factor in Bohr magnetons.[10] Thus, for the $5d[\frac{7}{2}]_4$ state of ^{129}Xe with spin $I = \frac{1}{2}$, $g_{9/2} = 1.1523$, and $g_{7/2} = 1.3897$. The frequency ν_F of a $\Delta F = 0$, $\Delta m_F = \pm 1$ transition in low magnetic field H_0 is approximately

$$\nu_F = g_F(\mu_B/h)H_0 , \quad (6)$$

where $\mu_B/h = 1.399\,61$ MHz/G. However, at higher magnetic fields the complete Hamiltonian for ^{129}Xe, combining the hyperfine structure and the Zeeman effect, is required:

$$\mathcal{H} = \mathcal{H}_{hfs} + \mathcal{H}_Z , \quad (7)$$

with

$$\mathcal{H}_{hfs} = ha\,\vec{I}\cdot\vec{J}$$

and

$$\mathcal{H}_Z = g_J\mu_B J_Z H_0 + g_I\mu_B I_Z H_0 .$$

The linear relationship of Eq. (6) between transition frequency and magnetic field is only correct for fields such that $\langle\mathcal{H}_Z\rangle \ll \langle\mathcal{H}_{hfs}\rangle$. As H_0 is increased, $\vec{I}$ and $\vec{J}$ decouple and the transition frequencies depart from linearity by an amount which depends not only on H_0, but also on the hfs constant a and the quantum numbers $(F, m_F \rightarrow F, m_F \pm 1)$ of the transition. Therefore, as the $F = \frac{9}{2}$ resonance was followed up to $H_0 = 100$ G, we observed it to split into two resonances, spaced almost symmetrically about the position given by Eq. (6). The separation of these two resonances was consistent with the value of the hfs constant $a = -582$ MHz measured by Liberman,[5] provided we assigned the $(m_F \rightarrow m_F - 1)$ quantum numbers $\frac{7}{2} \rightarrow \frac{5}{2}$ and $-\frac{5}{2} \rightarrow -\frac{7}{2}$ to the two transitions. These observations encouraged us to search for direct $(\Delta F = 1)$ hyperfine transitions to precisely determine a.

The $\Delta F = 1$ resonances required a transition frequency of about 2600 MHz and also successful coupling of the microwave rf field into the discharge region of the xenon diode. This was accomplished by means of the waveguide cavity and diode assembly outlined in Fig. 2. The TE_{102} mode cavity was driven by a phase-locked voltage-tuned magnetron and matched to the transmission line by a circular iris and waveguide to type-N adapter; the reference frequency for the phase-lock circuit was derived from the frequency synthesizer. For lock-in detection, the microwave power was square wave modulated by a PIN diode voltage-controlled attenuator.

The xenon discharge tube was constructed so that the anode-to-cathode spacing matched the narrow internal dimension of the waveguide cavity. The tube was located at the position of maximum amplitude of the microwave magnetic field. A number of small holes in the sides of the cavity allowed exit of light from the xenon discharge without destroying the cavity Q; the Q with the diode in position was about 100. The cavity resonant frequency could be tuned over a range of 50 MHz by means of a quartz tuning rod.

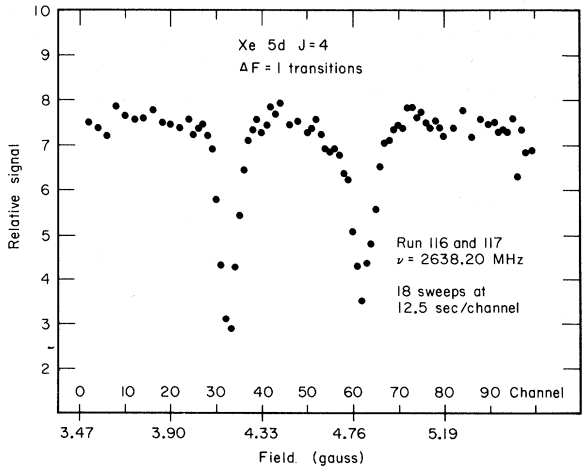

FIG. 6. Example of hfs resonances. The resonance on the left is the $(F = \frac{9}{2}, m_F = \frac{5}{2}) \rightarrow (\frac{7}{2}, \frac{7}{2})$ transition while the one on the right is the $(\frac{9}{2}, \frac{3}{2}) \rightarrow (\frac{7}{2}, \frac{5}{2})$ transition.

TABLE II. Summary of $\Delta F = 1$ observations.

Frequency (MHz)	Quantum numbers $F=\frac{9}{2} \rightarrow F=\frac{7}{2}$ m_F		Number of observations	Mean field of resonance centers (G)	Mean value of hfs constant a (MHz)
2638.200	$\frac{5}{2}$	$\frac{7}{2}$	8	4.168	−583.570(5)
2638.200	$\frac{3}{2}$	$\frac{5}{2}$	8	4.798	−583.573(4)
2613.800	$-\frac{3}{2}$	$-\frac{5}{2}$	7	4.862	−583.568(4)
2613.800	$-\frac{5}{2}$	$-\frac{7}{2}$	7	4.221	−583.572(5)

Figure 6 is a plot of two of the $\Delta F = 1$ resonances observed using the cavity and signal averaging system. The resonance frequency was fixed while the magnetic field was swept during all the $\Delta F = 1$ measurements. Each point in the plot required 225 sec of integration time. As expected, the $\Delta F = 1$ resonances are considerably weaker than the g_J resonances in the even-mass isotopes. This is primarily because only two out of $(2I+1)(2J+1) = 27$ sublevels participate in each ^{129}Xe $5d[\frac{7}{2}]_4$ $\Delta F = 1$ resonance, whereas in the even isotopes all sublevels can participate. The resonances shown in Fig. 6 were observed at a frequency of 2638.200 MHz; a second pair was observed while sweeping the same magnetic field region at a resonance frequency of 2613.800 MHz. Table II summarizes the $\Delta F = 1$ resonance observations. As in the g_J measurements, the magnetic field was calibrated using the $6s[\frac{3}{2}]_2$ metastable state resonance.

The frequencies and fields of the resonance centers of all 30 observations were fit by a computer routine which diagonalized the complete Hamiltonian $\mathcal{H} = \mathcal{H}_{hfs} + \mathcal{H}_Z$ and varied the hfs constant a to give the best least-squares fit to the data. The m_F quantum numbers listed in Table II were determined by the requirement that each of the four resonances observed yield consistent values for a; this gives a unique assignment. Our result for the hfs constant of the $5d[\frac{7}{2}]_4$ state of ^{129}Xe is $a = -583.571(2)$ MHz. The error is one standard deviation from the computed mean; it corresponds to approximately one-tenth the resonance linewidth.

ACKNOWLEDGMENTS

We are grateful for the advice of Dr. T. Hadeishi during construction of the hot-cathode discharge tube and for the assistance and encouragement of Professor H. A. Shugart throughout the experiment.

†Work supported by U. S. Atomic Energy Commission.

[1]H. G. Dehmelt, Phys. Rev. 103, 1125 (1956).
[2]W. E. Lamb, Jr., Phys. Rev. 105, 559 (1957).
[3]J. C. Pebay-Peyroula, in *Physics of the One- and Two-electron Atoms*, edited by F. Bopp and H. Kleinpoppen (North-Holland, Amsterdam, 1969), p. 348 ff.
[4]M. Chenevier, Compt. Rend. 268B, 1179 (1969).
[5]M. S. Liberman, Compt. Rend. 266B, 236 (1968).
[6]H. R. Schlossberg and A. Javan, Phys. Rev. Letters 17, 1242 (1966).
[7]H. Friedburg and H. Kuiper, Naturwiss. 44, 487 (1957).
[8]Obtained from Spectra-Mat, Inc., 1240 Highway 1, Watsonville, Calif. 95076.
[9]R. S. Van Dyck, Jr., C. E. Johnson, and H. A. Shugart, Lawrence Berkeley Laboratory Report No. LBL-18 (unpublished); this issue, Phys. Rev. A 5, 971 (1972).
[10]G. H. Fuller and V. W. Cohen, Nucl. Data Tables 5, 433 (1969).